

Experimental Rarefied Aerodynamic Forces at Hypersonic Conditions over 70-Degree Blunted Cone

J. Allègre,* D. Bisch,† and J. C. Lengrand‡

Centre National de la Recherche Scientifique, 92190 Meudon, France

The blunted cone has been chosen as a test case model to provide both experimental and computational databases in the field of hypersonic and rarefied flow conditions. Some preliminary results have already been presented at the Fourth European High-Velocity Database Workshop; the present work, focused on aerodynamic forces, gives a complete set of experimental data. Experiments have been conducted in the SR3 facility at a freestream Mach number close to 20 and for Reynolds numbers ranging from 1522 to 34,855, calculated using freestream conditions and the model base diameter. Aerodynamic forces and moments are presented for three levels of flow rarefaction and for model angles of attack between 0 and 30 deg. In parallel with the experimental work, flow calculations were made by an international group of researchers for identical test conditions. Examples of comparisons between experimental and computational aerodynamic forces are also indicated.

Nomenclature

A	= base area of the model, $\pi d^2/4$, m ²
C_A	= axial force coefficient
C_D	= drag coefficient, $D/0.5\rho AV^2$
C_l	= lift coefficient, $L/0.5\rho AV^2$
C_m	= pitching moment coefficient, $M/0.5\rho AdV^2$
C_N	= normal force coefficient
D	= drag, N
d	= base diameter, 50 mm
L	= lift, N
M	= pitching moment, mN
Ma	= nominal freestream Mach number
Ma_{mv}	= mean value of Mach number upstream of the model
Ma_{ref}	= reference freestream Mach number at the model nose
p_0	= stagnation pressure, bar
R_C	= corner radius, mm
Re_d	= Reynolds number calculated on the base diameter
R_n	= nose radius, mm
T_0	= stagnation temperature, K
V	= rarefaction parameter, $Ma/(Re_d)^{0.5}$
X_{CP}/L	= center-of-pressure abscissa measured from the model nose
α	= angle of attack, deg
ρ_∞	= freestream density, kg/m ³

Introduction

HYPERSONIC flows where rarefaction effects are important occur over a wide spectrum of space conditions that concern the overall aerodynamics of space vehicles flying at high-altitude and re-entry conditions. A companion paper is focused on the presentation of experimental density flowfields around and in the wake region of the blunted cone.¹ This paper provides experimental data on aerodynamic forces applied to the cone model with the objective of characterizing the effect of rarefaction on the exerted forces. The experimental values of the aerodynamic forces and moments are also available for purposes of code validation by means of comparisons with computational data.

As part of AGARD, the Fluid Dynamic Panel and its Working Group 18 have chosen the 70-deg spherically blunted cone as the

test case model. The forebody configuration is identical to that of the Mars Pathfinder probe. Some experimental data have been presented to the Fourth European High-Velocity Database Workshop.² The present paper includes the complete set of aerodynamic forces obtained through experiments performed at rarefied hypersonic conditions in the SR3 wind tunnel.

Test conditions are characterized by a freestream Mach number close to 20 and by Reynolds numbers ranging from 1522 to 34,855, calculated using freestream conditions and the cone base diameter. Aerodynamic forces and moments are measured for three wind-tunnel conditions and six cone angles of attack spanning 0 and 30 deg.

Cone Model and Aerodynamic Balance

The model is an axisymmetric, spherically blunted cone mounted on a cylindrical sting. To minimize the model weight and make its mounting easier on the external balance, the blunted cone and the sting are made of aluminum alloy. Cone base and sting diameters are 50 and 12.5 mm, respectively. The sting length represents three times the cone base radius. All dimensions of the model are given in Fig. 1.

The balance, schematically presented in Fig. 2, has been designed specifically for the SR3 test section within the framework of previous contracts with Hughes Aircraft and Aerospatiale. The balance provides direct measurements of drag, lift, and pitching moment and indirect determination of the center of pressure. As indicated in Fig. 2, the model is connected to the balance by means of two tungsten wires, 0.2 mm in diameter. One horizontal wire, tightened on a circular frame, passes through the model in its front region, and one vertical wire leads to a thin needle screwed on the rear extremity of the cylindrical sting. Basically, the balance consists of three separate dynamometers. The lift acts on the two dynamometers indicated at the top of Fig. 2, whereas the drag acts on a third dynamometer composed of two separate elements located on either side of the test section. The circular frame, which surrounds the test section, provides the tension of the horizontal wire and transmits both the drag and the front lift components to the respective dynamometers. The rear lift component is transmitted by means of the vertical link wire. When performing the measurements, to eliminate wire effects, the drag of the horizontal wire only is measured and then subtracted from the total drag measured with the model. The drag of the vertical wire is neutralized by enclosing the wire within a fairing. Also, to avoid any interaction between the nozzle flow and the circular frame of the balance, a removable cylindrical screen is introduced between the test section and the circular frame.

Test Facility and Flow Conditions

The SR3 wind tunnel is equipped with pumping systems working in continuous operation. According to the required flow conditions and to the rarefaction level, two distinct pumping groups are used.

Received Jan. 9, 1997; revision received July 3, 1997; accepted for publication July 11, 1997. Copyright © 1997 by the American Institute of Aeronautics and Astronautics, Inc. All rights reserved.

*Research Engineer, Department of Hypersonics and Rarefied Flow, 4 ter route des Gardes.

†Research Assistant, Department of Hypersonics and Rarefied Flow, 4 ter route des Gardes.

‡Head, Laboratoire d'Aérodynamique, 4 ter route des Gardes. Member AIAA.

At the lowest flow densities (conditions 1 and 2), the exhaust system is composed of rotary piston vacuum pumps, Roots pumps, and oil diffusion booster pumps, withstanding volume flow rates of air or nitrogen of about 40 m³/s under working pressures up to 10⁻⁴ atm. At higher flow densities (condition 3), the exhaust system includes rotary sliding vane pumps and Roots pumps.

Force measurements are performed at hypersonic and rarefied flow conditions for three rarefaction levels, which with the nominal operating conditions are indicated in Table 1. Nitrogen flows

Table 1 SR3 wind tunnel experimental test conditions						
Flow conditions	Gas	Ma	T ₀ , K	p ₀ , bars	Re _d	\tilde{V}
1	N ₂	20.2	1,100	3.5	1,420	0.53
2	N ₂	20.1	1,100	10	4,116	0.31
3	N ₂	20.9	1,300	120	34,263	0.11

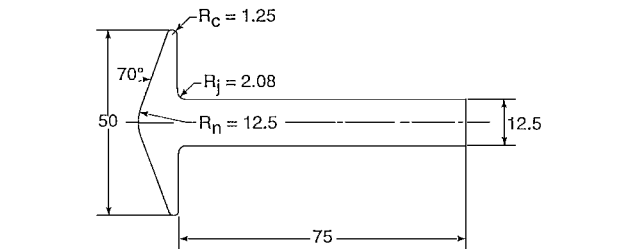


Fig. 1 Light alloy test model for force measurements. All dimensions are in millimeters.

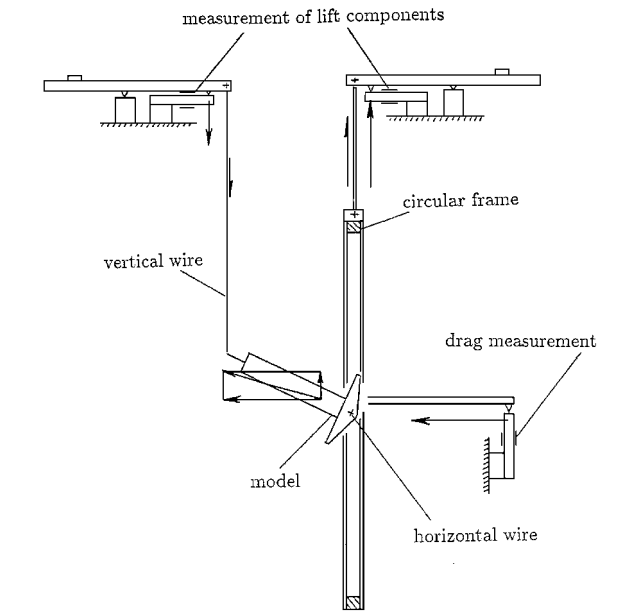


Fig. 2 Schematic representation of the external balance.

are issued from three different nozzles supplied with an electrical graphite heater. Divergent sections of the nozzles are conical and continued by cylindrical extensions providing the junction between the conical parts and the test section. Reynolds numbers Re_d and rarefaction parameters [$\tilde{V} = Ma/(Re_d)^{0.5}$] have been calculated assuming, as a reference, the 5-cm-cone base diameter. The Sutherland viscosity law is applied for gas temperatures down to 100 K, and then a linear viscosity law is used at lower gas temperatures between 0 and 100 K. The flow parameters are assumed to take their nominal values at the nose location of the blunted cone.

At high Mach numbers and rarefied flow conditions, the use of nozzles with conical divergent sections results in the existence of transverse and longitudinal density gradients through the test section.¹ To take into account transverse freestream Mach gradients just ahead of the blunted cone, mean values of Mach number Ma_{mv} have been calculated by averaging freestream Mach number distributions over the front diameter of the blunted cone. These Mach numbers are slightly different from nominal Mach numbers. As indicated in Fig. 3, for the three flow conditions investigated, mean values of Mach number Ma_{mv} are 19.75, 20.3, and 20.8, whereas nominal Mach numbers are 20.2, 20.1, and 20.9, respectively. Corresponding values of Reynolds numbers are then 1522, 4010, and 34,855, respectively.

From aerodynamic forces measured with the balance, aerodynamic coefficients have been calculated using mean values of Mach number ahead of the blunted cone. The reference area corresponds to the base cross section ($A = \pi d^2/4$), and the reference length is the cone base diameter. The origin for presenting the center-of-pressure abscissa is the nose of the model. Because of the model protection prior to the measurements, and also considering the period of time limited to a few tens of seconds required for force measurements, the wall temperature of the model does not increase more than 50 K during the run. As a mean value, the wall temperature is estimated to be close to 350 K at the time of the measurement.

Force Measurement and Test Procedure

At rarefied and hypersonic test conditions, the blunted shape of the model makes the establishment of nozzle flow difficult when the model is initially located through the test section. Consequently, a mechanical device has been added to the balance to improve the flow starting, as well as to protect the model from the shocks generated when starting or shutting down the nozzle flow. The mechanical device is mainly composed of a sharp cone, mounted at the extremity of a streamlined support, which is injected just upstream of the blunted cone before the starting or shutting processes. Details of the procedure used to measure aerodynamic forces are given in Ref. 3.

Prior to force measurements, the three dynamometers of the balance have been calibrated by means of weights of known values. Because of the level of measured forces, calibration has been made with weights ranging from 0 to 100 g for the drag dynamometer and with weights ranging from 0 to 50 g for the two lift dynamometers. Successive calibrations have shown a good repeatability of the measurements, as well as a linear variation between output signals and applied forces. Strain gauge bridges mounted on the three dynamometers of the balance are connected to an HBM System,

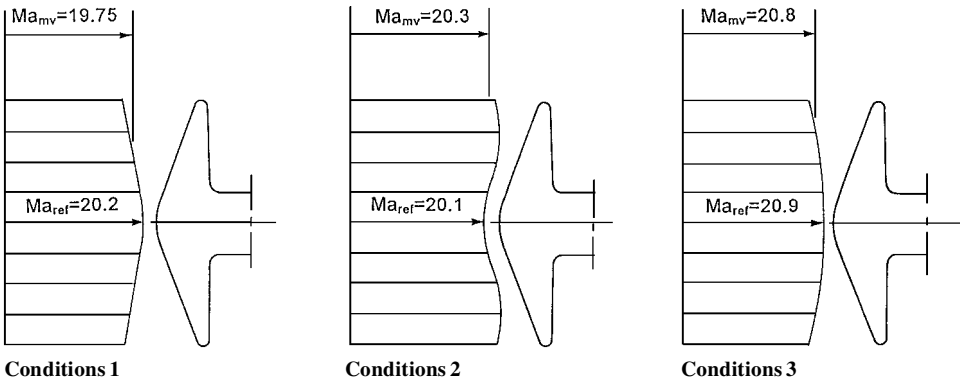


Fig. 3 Upstream flow gradients.

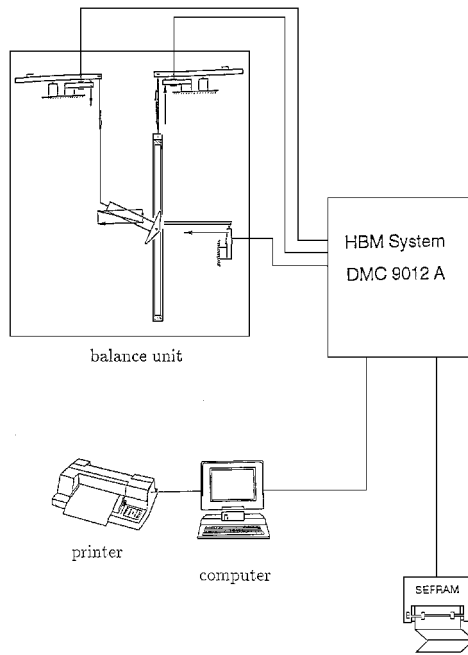


Fig. 4 Measurement setup.

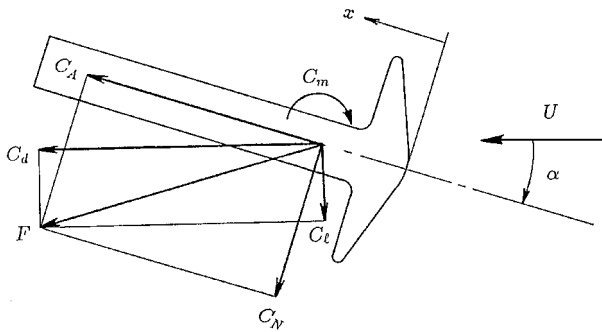


Fig. 5 Definition of force coefficients.

DMC 9012 A, like that shown in Fig. 4. The HBM unit, controlled by microprocessor, includes a multiple-channel measuring amplifier system. All amplifier units are connected in parallel, via a data and control bus, with the central processing unit. The HBM system is operated via a personal computer, also used for data acquisition and data reduction. Output signals coming from strain gauge bridges are also applied to a galvanometer recording unit, SEFRAM. Balance signals are then recorded during all force measurements and are verified in case of any experimental difficulty.

Experimental Data

All results are summarized in Tables 2-4. Data are presented for three flow rarefaction levels and six angles of attack of the blunted cone, including angles of drag and lift coefficients, pitching moment coefficients, axial force and normal force coefficients, and centers of pressure.

The force and moment coefficients with positive orientations are specified in Fig. 5. The point of restitution for the pitching moment corresponds to the nose of the blunted cone. The center-of-pressure abscissa X_{CP}/L is measured along the model axis downstream from the nose location. L represents a reference length equal to the base diameter of the blunted cone ($d = 50$ mm).

Aerodynamic coefficients have been plotted vs the angle of attack for the three rarefaction levels. Drag and lift coefficients, as well as axial force and normal force coefficients, are presented in Figs. 6-9. The axial force coefficient is maximum at 0-deg angle of attack and decreases continuously when angles are increased from 0 to 30 deg. At the present conditions covering continuum and transitional flow regimes, and considering a same angle of incidence, the axial force coefficient increases with higher rarefaction levels. Distributions of

Table 2 Aerodynamic coefficients (test conditions 1: $Ma = 19.75, Re_d = 1522$)

α , deg	C_D	C_l	C_m	C_A	C_N	X_{CP}/L
0	1.657	0	0	1.657	0	
5	1.629	-0.057	-0.058	1.628	0.084	0.691
10	1.615	-0.133	-0.079	1.614	0.148	0.534
15	1.569	-0.200	-0.133	1.568	0.213	0.627
20	1.538	-0.249	-0.185	1.530	0.291	0.635
30	1.432	-0.324	-0.304	1.402	0.434	0.699

Table 3 Aerodynamic coefficients (test conditions 2: $Ma = 20.3, Re_d = 4010$)

α , deg	C_D	C_l	C_m	C_A	C_N	X_{CP}/L
0	1.520	0	0	1.520	0	
5	1.511	-0.093	-0.019	1.514	0.038	0.503
10	1.476	-0.180	-0.054	1.485	0.078	0.683
15	1.438	-0.254	-0.093	1.455	0.126	0.736
20	1.356	-0.309	-0.127	1.380	0.172	0.736
30	1.208	-0.369	-0.224	1.231	0.283	0.791

Table 4 Aerodynamic coefficients (test conditions 3: $Ma = 20.8, Re_d = 34,855$)

α , deg	C_D	C_l	C_m	C_A	C_N	X_{CP}/L
0	1.501	0	0	1.501	0	
4.3	1.494	-0.087	-0.025	1.497	0.025	1.032
9.8	1.448	-0.197	-0.060	1.460	0.051	1.156
15.3	1.381	-0.275	-0.090	1.405	0.099	0.910
20.3	1.298	-0.339	-0.123	1.335	0.131	0.933
29.6	1.127	-0.400	-0.190	1.178	0.208	0.911

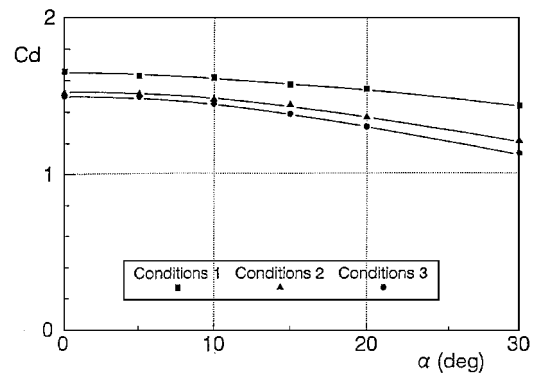


Fig. 6 Drag coefficient.

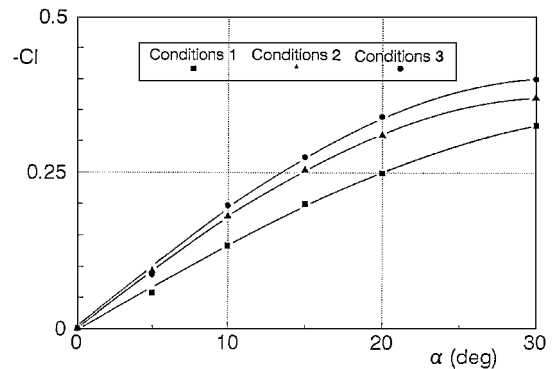


Fig. 7 Lift coefficient.

the normal force coefficient point out the increase of the coefficient for higher angles of incidence and for more rarefied flow conditions. Pitching moment coefficients and center-of-pressure locations also represent useful information to predict the dynamic stability of the model (Figs. 10 and 11). The center of pressure is found to be closer to the model nose with the most rarefied flow conditions, whereas it does not seem to be noticeably affected by the variation of the angle of attack.

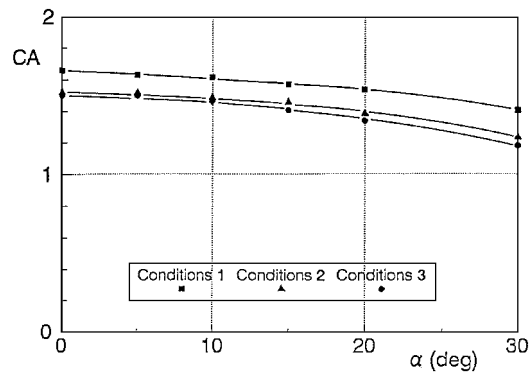


Fig. 8 Axial-force coefficient.

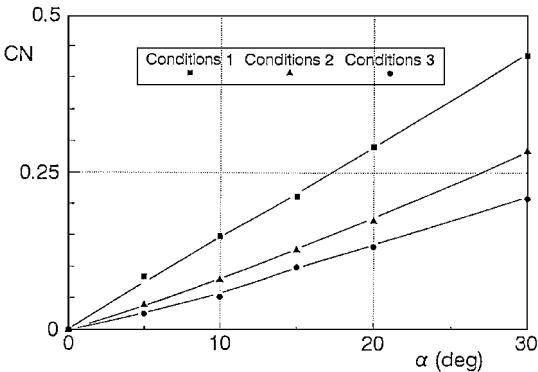


Fig. 9 Normal-force coefficient.

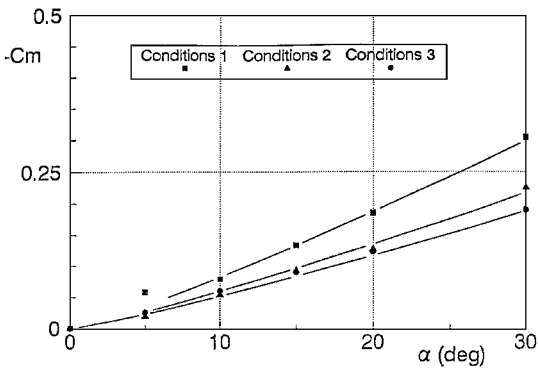


Fig. 10 Pitching-moment coefficient.

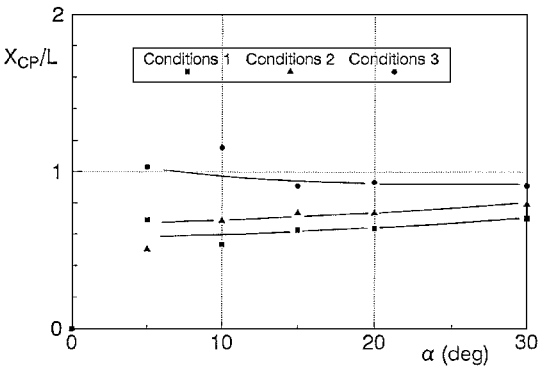


Fig. 11 Center of pressure.

The present experimental results represent a contribution to a database specific for hypersonic conditions. The blunt-body problem has been studied for high-enthalpy tests obtained with impulse facilities^{4,5} and for rarefied tests^{1,6} performed in rarefied low-enthalpy facilities. In parallel to the present experimental work, a number of calculations using a direct simulation Monte Carlo solution (DSMC) were executed by an international group of researchers. An extensive number of computations have been made

Table 5 Calculated and measured drag coefficients for SR3 test conditions

Test conditions	Drag coefficients	
	Calculated (Moss et al. ⁸)	Measured (SR3)
1	1.69	1.66
2	1.62	1.52
3	1.57	1.50

over the blunted cone for SR3 test conditions because it was one of the test cases at the Fourth European High-Velocity Database Workshop. Some results were included at the workshop and were indicative of the good agreement achieved between computation and experiment.^{2,7}

A number of comparisons between computed aerodynamic forces and experimental aerodynamic forces have already been presented.^{7–9} To illustrate force comparisons, Table 5 shows, for the blunted cone at 0-deg angle-of-attack, drag coefficients calculated by Moss et al.⁸ and drag coefficients measured in the SR3 wind tunnel. Maximum differences of 6% are found between measured and DSMC calculated drag coefficients.

Accuracy of the Measurements

Data uncertainty may result from different causes: uncertainty in the measurement of the model angle of attack, uncertainty in the definition of flow conditions ahead of the model, and uncertainty related to the balance alignment and to its calibration.

The angle of incidence of the model is measured optically during the run with an uncertainty of the order of ± 0.1 deg, the upper limit being ± 0.15 deg when slight oscillations of the model reduce the clarity of the optical reading.

An uncertainty in the definition of flow conditions may also lead to a correlative uncertainty in the indicated values of force and moment coefficients. This comes from the dependence of the dynamic pressure with the freestream Mach number. As an example, increasing the Mach number from 20 to 20.1 leads to a correlative increase of about 2.3% in the force and moment coefficients. Assuming for the freestream Mach number a relative uncertainty $\Delta Ma/Ma = \pm 0.5\%$, values of aerodynamic coefficients are then characterized by uncertainties less than $\pm 2.5\%$. Such uncertainties are realistic when mean values of Mach number ahead of the model are taken into account to calculate aerodynamic coefficients.

Concerning the balance itself, the correct location of its mechanical components is optically verified prior to the balance calibration. Then, calibration consists in measuring signal deviations of drag, front lift, and rear lift when applying known forces. The uncertainty concerns the measurement of the signal amplitudes. Practically, the repetition of the measurements is excellent and calibration uncertainty is less than $\pm 0.5\%$. Consequently, values of aerodynamic coefficients are presented with a global uncertainty that should not exceed about $\pm 3\%$.

Concluding Remarks

At rarefied and hypersonic conditions, experiments have been conducted in the SR3 wind tunnel on a blunted cone test model. Experimental results are focused on aerodynamic forces under conditions characterized by a freestream Mach number close to 20 and three levels of gas rarefaction. Reynolds numbers, calculated using freestream conditions and the cone base diameter, range from 1522 up to 34,855. Aerodynamic forces were measured for each flow condition at six angles of incidence spanning 0 and 30 deg. Presented aerodynamic data include drag and lift coefficients, axial and normal force coefficients, pitching moment coefficients, and center-of-pressure location. The investigation gives information on rarefaction effects and makes experimental results available for the primary purpose of allowing comparisons with computational data.

Acknowledgments

This work was supported by the European Space Agency (ESA-ESTEC) under Contracts 132622 and 133790.

References

- ¹Allègre, J., Bisch, D., and Lengrand, J. C., "Experimental Rarefied Density Flowfields at Hypersonic Conditions over 70-Degree Blunted Cone," *Journal of Spacecraft and Rockets*, Vol. 34, No. 6, 1997, pp. 714-718.
- ²Coron, F., and Harvey, J. K., "Synopsis for Test Case 6—Rarefied 70 Degree Spherically Blunted Cone Flow," Fourth European High-Velocity Database Workshop, ESTEC, Noordwijk, The Netherlands, Nov. 1994.
- ³Allègre, J., and Bisch, D., "Blunted Cone at Rarefied Hypersonic Conditions—Experimental Density Flowfields, Heating Rates and Aerodynamic Forces," Laboratoire d'Aérodynamique, Rept. RC 95-2, Centre National de la Recherche Scientifique, Meudon, France, Sept. 1995.
- ⁴Gochberg, L. A., Allen, G. A., Gallis, M. A., and Deiwert, G. S., "Comparison of Computations and Experiments for Nonequilibrium Flow Expansions Around a Blunted Cone," AIAA Paper 96-0231, Jan. 1996.
- ⁵Holden, M., Harvey, J., Boyd, I., George, J., and Horvath, T., "Experimental and Computational Studies of the Flow over a Sting Mounted Planetary Probe Configuration," AIAA Paper 97-0768, Jan. 1997.
- ⁶Danckert, A., and Legge, H., "Wake Structure of a 70 Degree Blunted Cone, DSMC Results and Patterson Probe Measurements," AIAA Paper 95-2141, June 1995.
- ⁷Moss, J. N., Price, J. M., and Dogra, V. K., "DSMC Calculations for a Spherically Blunted Cone," Fourth European High-Velocity Database Workshop, ESTEC, Noordwijk, The Netherlands, Nov. 1994.
- ⁸Moss, J. N., Price, J. M., Dogra, V. K., and Hash, D. B., "Comparison of DSMC and Experimental Results for Hypersonic External Flows," AIAA Paper 95-2028, June 1995.
- ⁹Moss, J. N., and Price J. M., "Review of Blunt Body Wake Flows at Hypersonic Low Density Conditions," AIAA Paper 96-1803, June 1996.

I. D. Boyd
Associate Editor